

## Diffuse Mössbauer Scattering Applied to Dynamics of Phase Transformations

B. W. Batterman,\* G. Maracci, A. Merlini, and S. Pace

*Solid State Physics Division, EURATOM, Ispra, Italy*

(Received 4 June 1973)

Bcc Zr-20% Nb has a lattice instability, forming the so-called hexagonal  $\omega$  phase. We show that it is possible to measure diffusely scattered Mössbauer  $\gamma$  rays associated with this transformation and determine whether this scattering is energy shifted. The results strongly suggest a dynamical aspect to the transformation and indicate that Mössbauer scattering can be a significant complement to inelastic neutron diffraction techniques.

There is much current work on inelastic scattering effects associated with phase transformations. Most of this effort is with inelastic neutron scattering techniques and concerns the detection of mode softening. With care, conventional triple-axis neutron inelastic scattering can be done with resolutions that approach about  $10^{-5}$  eV and in special cases as high as  $10^{-6}$  eV.

Mössbauer scattering can, in principle, detect inelastically scattered  $\gamma$  rays shifted by energies as small as  $10^{-8}$  eV. It has been shown<sup>1,2</sup> that thermal diffuse scattering (TDS) in the close vicinity of Bragg reflections (i.e., due to long-wavelength phonons) can be separated from the elastically scattered Bragg reflections, and the measured total TDS intensity agrees well with that calculated from elastic constants. For small phonon vectors  $\vec{q}$ , i.e., scattering in the vicinity of the zone center, the TDS is quite strong; the Mössbauer resonance absorption allows easy separation of the TDS which is shifted on the order of a few meV from the elastic scattering.

In this work we demonstrate that diffuse scattering from a Mössbauer source can be measured in regions in the middle of the Brillouin zone, away from the zone centers, and can be separated into elastic and inelastic components.

When Nb is added to Zr, the hexagonal phase of the latter is suppressed. For samples of Zr-20% Nb quenched from high temperature, the alloy remains bcc with a tendency to form a hexagonal  $\omega$  phase. This tendency manifests itself in intense diffuse scattering which is strongest in the vicinity of the hexagonal reciprocal-lattice points of the  $\omega$  phase. Our work was prompted by the findings of Moss, Keating, and Axe,<sup>3</sup> who reported that the diffuse scattering at the  $\omega$  positions described above is elastic to the limits of their detectability, i.e., to about  $10^{-6}$  eV with inelastic neutron diffraction techniques.

The principle of the Mössbauer experiment is straightforward and is outlined in detail else-

where.<sup>1,2</sup> In simplest terms, one measures the scattered Mössbauer  $\gamma$  rays with and without a resonant absorber between the sample and the detector. That portion of the  $\gamma$  rays scattered inelastically, losing energies greater than the Mössbauer resonance width ( $\approx 2 \times 10^{-8}$  eV), will have a much smaller attenuation in the resonant absorber. In order to correct for the 120-keV  $\gamma$  rays associated with the decay of the excited nuclear level of Fe<sup>57</sup>, additional measurements of the scattered intensity are made with a thick aluminum absorber between the source and detector. The aluminum completely absorbs the 14.4-keV Mössbauer line, and the intensity measured in this case is used to correct the data for scattering associated with the 120-keV  $\gamma$  rays. Thus, for a given scattering vector  $\vec{k} - \vec{k}_0$  ( $\vec{k}$  and  $\vec{k}_0$  are the scattered and incident wave vectors, respectively), four measurements are made, i.e., all combinations of the Mössbauer and aluminum absorbers in and out. A thin lamella of RbCl single crystal placed in front of the counter was used to cut down the Nb and Zr fluorescence scattering for all measurements.

In order to have an appropriate road map of diffuse scattering in the reciprocal lattice, we measured the scattering in the  $(\bar{1}10)$  plane of the bcc reciprocal lattice with conventional x-ray techniques. We used Mo  $K\alpha$  radiation monochromatized by a singly bent quartz crystal. The intensity of the incident beam was monitored by a periodic check of the scattering from a block of Lucite.

Figure 1 illustrates the diffuse x-ray scattering from a single crystal of Zr-20% Nb quenched from 1000°C into oil. The sample was provided by Sass, and was treated in the same way as specimens used in electron-microscopy studies<sup>4</sup> which helped characterize the  $\omega$  phase diffuse scattering. The contours in Fig. 1 are uncorrected for polarization or atomic scattering factors and are observed directly in cycles per second. The volume of reciprocal space illuminated (i.e.,

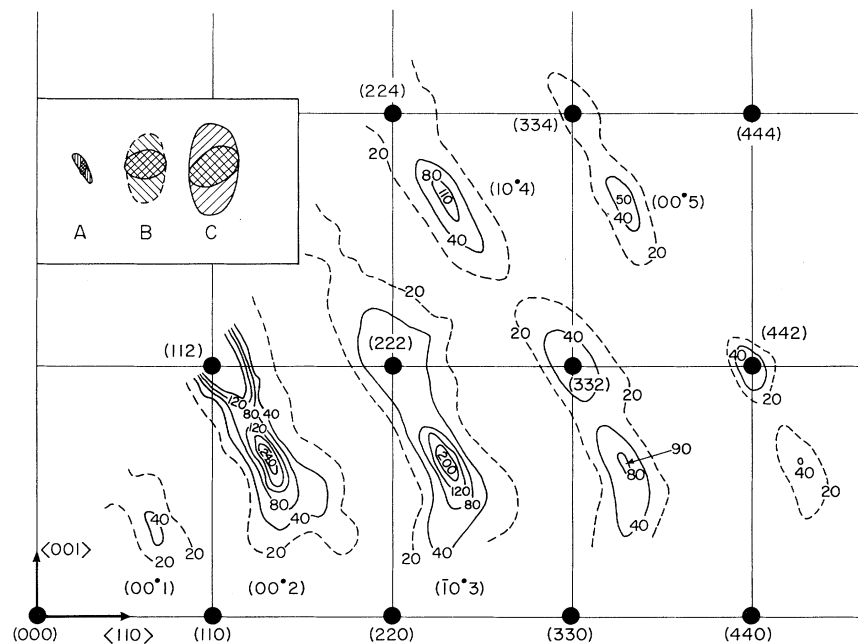


FIG. 1. X-ray scattering in the  $(\bar{1}10)$  plane of the bcc reciprocal lattice of Nb(20% Zr). Intensity contours are in observed cycles per second. In the inset, *A* is the resolution volume used in the x-ray measurement. The cross-hatched area is the section of the resolution volume in the plane of the figure, and the large singly hatched area is for the section normal to the figure. The outer contour corresponds to a level  $\frac{1}{5}$  of the maximum. Insets *B* and *C* are the corresponding volumes used in the Mössbauer scattering experiments.

volume element or resolution volume) is indicated in inset *A* for the plane of the figure, as well as for the plane normal to it. The resolution volume was determined experimentally by using the Bragg reflection of a perfect silicon crystal to trace out the scattered Bragg intensity. The volume element is determined almost entirely by the incident and scattered beam divergences. The diffuse peaks and the plot in general are in good agreement with neutron measurements.<sup>3</sup> These differ from electron-diffraction results<sup>4</sup> because the latter are subject to strong multiple scattering effects. However, the qualitative shape and shift of the diffuse peaks from the exact hexagonal positions are the same as in the electron-diffraction patterns.

The main problem in the Mössbauer measurement is that of low intensity. Our approach was to use the map of Fig. 1 as a guide, and to increase the size of the volume element as much as possible and still be able to resolve the diffuse peaks from the Bragg reflections.

The inset in Fig. 1 gives an idea of the approximate resolution volume used in the x-ray and the Mössbauer measurements. *B* and *C* are two Mössbauer volume elements, whereas *A* is the x-ray resolution. The outer contour of the el-

lipselike regions correspond to a level  $\frac{1}{5}$  of the maximum intensity. The shape of the element will depend to some extent on the position in reciprocal space, but the size will not change very much.

In Fig. 2 we show a Mössbauer scan along a  $\langle 111 \rangle$  direction encompassing the  $(00.2)$   $\omega$  diffuse and the  $(222)$  bcc Bragg reflections using resolution volume *B* as shown in Fig. 1. At the  $(00.2)$  position we see a well-defined inelastic peak essentially coincident in position with an elastic portion. The relative peak heights of elastic to inelastic (above the inelastic background) is about 4, i.e., the inelastic is about 25% of the elastic. At the  $(222)$  Bragg position the inelastic peak corresponds to TDS from the matrix as well as to an inelastic contribution of an  $\omega$ -phase diffuse peak at the point. In Fig. 3 are the corresponding curves through the  $\omega$  diffuse  $(00.5)$  and  $(10.4)$  reflections using resolution volume *C*. The *B* volume was obtained by reducing the incident and receiving slit areas by factors of 2.5 and 2.9, respectively, over that used for *C*. The intensity was reduced about a factor of 6 in the process. The curve of the  $(00.2)$  using the larger resolution volume had a greater inelastic-to-elastic peak ratio ( $\approx 32\%$ ). This is most probably because of

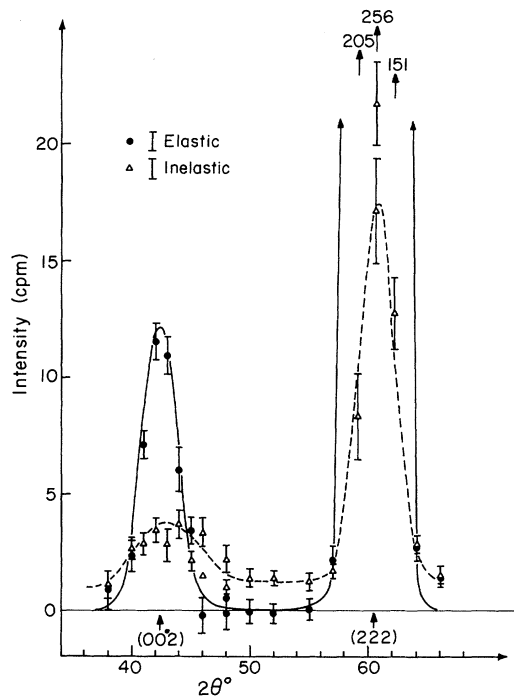


FIG. 2. Inelastic and elastic Mössbauer scattering along a  $\langle 111 \rangle$  direction using resolution volume  $B$  in Fig. 1. This corresponds to a run along the radial direction between (000) and (222) in Fig. 1.

the poorer resolution volume encompassing a greater portion of the inelastic background and possibly because of some of the TDS under the (222). The inelastic-to-elastic peak ratios are 50% and 75% for (10.4) and (00.5), respectively. The inelastic fraction clearly increases for diffuse  $\omega$  peaks further out in reciprocal space.

It is clear from these measurements that the  $\omega$  diffuse reflections are not totally elastic, but have a fraction of inelastic component which increases with increasing diffraction vector. If the inelastic peaks were merely thermal scattering from the matrix, we would expect the same intensity at symmetry related points. For example, the (00.4) position halfway between (222) and (00.5) (see Fig. 1) is equivalent to the (00.2) position. Thermal scattering is proportional to  $F^2 \times |S|^2 P e^{-2M}$ , where  $F$  is the effective atomic scattering factor,  $S$  the length of the diffraction vector,  $P$  the polarization factor, and  $e^{-2M}$  the Debye-Waller factor. We estimate the ratio of TDS between (00.4) and (00.2) to be 1.2. Using the 25% figure for the inelastic-elastic ratio at (00.2), we estimate that the x-ray count (Fig. 1) at the (00.4) position due to TDS should be about 60 units. The contour at the (00.4) is less than 20 units, and an

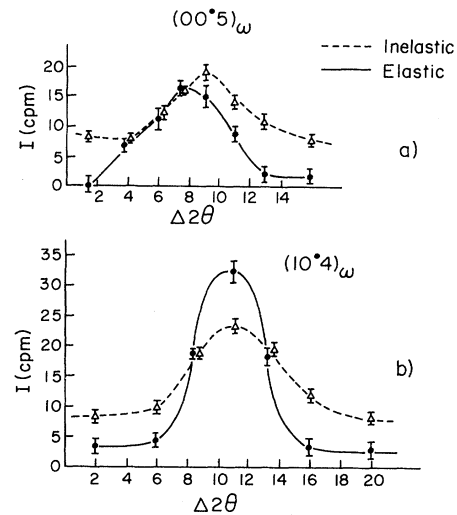


FIG. 3. Same as in Fig. 2 (using resolution volume  $C$  in Fig. 1) in the vicinity of (a) the (00.5) and (b) the (10.4)  $\omega$  diffuse peaks. Both curves are radial runs in reciprocal space.

appreciable fraction of this intensity is due to Compton scattering. Furthermore, we see no hint of any peak at (00.4). We can conclude with a fair measure of certainty that the inelastic peaks seen with the Mössbauer measurements are not thermal diffuse scattering from the matrix but are inherent in the phenomenon that causes the  $\omega$  diffuse scattering.

We have made preliminary measurements of the (00.2) diffuse peak as a function of temperature with conventional x rays and with  $\text{Fe}^{57}$  Mössbauer  $\gamma$  rays. Between room temperature and liquid  $\text{N}_2$  the (00.2) increased 35% in average intensity. At the low temperature the peak shape was somewhat narrower than at room temperature but the difference was less than 10%. The intensity changes in this temperature range were reversible, and there did not appear to be an  $\omega$ -start temperature curve below which a hexagonal phase precipitates.

The Mössbauer results with the resolution volume used for low-temperature measurements show that the inelastic/elastic ratio decreased from about 25% at room temperature to about 10% at 77°K. There are two principal results to be derived from this preliminary study. The first is an experimental demonstration that the diffuse scattering associated with a possible lattice instability can be measured and that this scattering can be separated into elastic and inelastic fractions with a resolution of about  $2 \times 10^{-8}$  eV. The technique should provide a significant comple-

ment to neutron diffraction techniques applied to transformations in which soft-mode behavior is suspected.

As for the  $\omega$  phase in ZrNb it can be definitely concluded that there are dynamical aspects to the instability towards the formation of the  $\omega$  phase. The diffuse scattering could not result solely from static distributions of small  $\omega$ -phase particles. One can only speculate on the source of the inelastic scattering. One possibility is that local regions of the bcc matrix fluctuate so that the atomic configuration resembles the hexagonal  $\omega$  phase, and that in time this dissolves away and the hexagonal-like fluctuation appears in another region of the crystal.

Another possibility is that hexagonal-like regions behave as very small crystallites which have the vibrational modes of a relatively large unit, and it is scattering from this vibrating unit

that results in inelastic scattering.

We are particularly indebted to Professor S. Sass for providing the specimens, and to Dr. D. Keating for helpful discussion. One of us (B.W.B.) wishes to express his gratitude to the John Simon Guggenheim Foundation for supporting this work.

---

\*Work supported by a grant from the John Simon Guggenheim Foundation. Permanent address: Department of Materials Science and Engineering, Cornell University, Ithaca, N.Y. 14850.

<sup>1</sup>C. Ghezzi, A. Merlini, and S. Pace, *Nuovo Cimento* **64B**, 103 (1969).

<sup>2</sup>G. Albanese, C. Ghezzi, A. Merlini, and S. Pace, *Phys. Rev. B* **5**, 1745 (1972).

<sup>3</sup>S. C. Moss, D. T. Keating, and J. D. Axe, *Bull. Amer. Phys. Soc.* **18**, 313 (1972).

<sup>4</sup>S. Sass, *J. Less-Common Metals* **28**, 157 (1972).

---

## Interband Masses of Higher Interband Critical Points in Ge

D. E. Aspnes

*Bell Laboratories, Murray Hill, New Jersey 07974*

(Received 15 May 1973)

Interband reduced masses for the critical points  $E_0$ ,  $E_0 + \Delta_0$ ,  $E_1$ ,  $E_1 + \Delta_1$ ,  $E_0'$ ,  $E_0' + \Delta_0'$ ,  $E_0' + \Delta_0' + \Delta_0$ , and  $E_2$  have been determined accurately for Ge from Franz-Keldysh oscillations. The observation of a well-defined interband reduced mass for the  $E_2$  structure suggests a relatively well-localized critical-point origin for this spectral feature, in contrast to presently accepted interpretations.

Although effective masses contain information about exchange and correlation effects<sup>1</sup> in addition to mutual interactions between bands well separated in energy, these parameters are generally neglected in energy-band theory principally because, with very few exceptions,<sup>2,3</sup> it has not been possible to obtain any direct information about them except in the vicinity of fundamental direct or indirect absorption edges. In this Letter, we report the first experimental measurement, for any material, of the interband reduced masses for a complete set of direct interband critical points up to and including the  $E_2$  transition. In addition to demonstrating that reduced masses of higher interband critical points are accessible to experimental investigation, these new results show that the  $E_2$  critical point in Ge has a well-defined interband reduced mass, which indicates a relatively well-localized contributing region in contrast to presently accepted interpre-

tations for this spectral feature in Ge and in other semiconductors.<sup>3-8</sup>

Interband reduced masses are determined here by means of subsidiary or Franz-Keldysh oscillations<sup>9</sup> which arise in the theory of electroreflectance (ER). These oscillations are not present in the low-field theory usually applicable to higher-interband transitions, but must be described mathematically by intermediate-field theory<sup>10</sup> which predicts

$$\frac{\Delta R}{R} \sim C_1(E) + \operatorname{Re} \left\{ C_2(E) e^{-Q(E)} \cos \left[ \frac{2}{3} \left( \frac{E - E_s}{\hbar \Omega} \right)^{3/2} + \theta_0 \right] \right\}. \quad (1)$$

Here,  $\Delta R/R = [R(\mathcal{E}_s) - R(0)]/R(0)$  is the usual modulated relative reflectance spectrum measured in ER;  $\mathcal{E}_s$  is the surface field; and  $C_1(E)$ ,  $C_2(E)$ ,  $Q(E)$ , and  $\theta_0$  are coefficients which vary slowly